Electronic Supplementary Material (ESI) for Energy & Environmental Science

α-Fe_2O_3 multi-shelled hollow microspheres for lithium ion battery anodes with superior capacity and charge retention

Simeng Xu,[a] *Colin M. Hessel,*[b] *Hao Ren,*[a] *Ranbo Yu,*[a,*] *Quan Jin,*[b] *Mei Yang,*[b] *Huijun Zhao, and Dan Wang,*[b,*]

[a] Department of Physical Chemistry, School of Metallurgy and Ecological Engineering, University of Science and Technology Beijing, Beijing 100083, PR China, E-mail: ranboyu@ustb.edu.cn

[b] State Key Laboratory of Multiphase Complex Systems, Institute of Process Engineering, Chinese Academy of Sciences, No. 1, Beierjie, Zhongguancun, Beijing 100190, P.R. China E-mail: danwang@mail.ipe.ac.cn

[c] Centre for Clean Environment and Energy, Gold Coast Campus, Griffith University, Queensland 4222, Australia.

Supporting Information

Experimental Section

Materials: Hydrated ferric nitrate ($Fe(NO_3)_3$•$9H_2O$, 99%), sucrose (98.5%), ethanol (98%), N-methylpyrrolidone (NMP 99.9%), Super P carbon black (99%), polyvinylidene fluoride (99%), and acetonitrile (99%) were purchased from *Beijing Chemical Co. Ltd.* and used as received.

Synthesis of multi-shell α-Fe_2O_3 hollow spheres: Carbonaceous microspheres were synthesized by the hydrothermal emulsion polymerization of sucrose as previously described.[1,2] In brief, 130 g of sucrose is dissolved in 250 mL of deionized (DI) water and heated to 200°C for 130 min in a sealed Teflon reactor. The brown product is washed 6 times alternatively with DI water and ethanol and dried at 80°C for 12 hr. The prototypical synthesis of triple-shell α-Fe_2O_3 hollow microspheres is as follows: 600 mg of newly prepared carbonaceous microspheres are dispersed by sonication in 30 mL of a 5 M ferric nitrate solution for 15 min and then stirred for 6 hr at room temperature. The mixture is filtered, washed once with DI water, and dried at 80°C for 12 hr. Hollow shell multi-spheres were produced by heating the infused carbonaceous microspheres to 500°C for 1 hr in a muffle furnace at a rate 2°C min^{-1}. The α-Fe_2O_3 hollow microspheres were collected as a deep red

powder. The thickness of the hollow microsphere shell was increased by increasing the ethanol content in the aqueous precursor infusion solution from 0% Ethanol, 33%, 66%, and 100%, while the washing, drying, and thermal processing steps remained unchanged. The complete set of experimental details can be found in Table S2.

Materials characterization: Scanning electron microscopy (SEM) images were obtained using a JSM-6700 microscope operating at 5.0 kV. Transmission electron microscopy (TEM) images were taken on a FEI Tecnai F20 instrument using an accelerating voltage of 200 kV. The SEM and TEM samples were prepared by drop-coating very dilute ethanol dispersions of hollow spheres onto copper foils and carbon-coated copper TEM grids, respectively. Powder X-ray diffraction (XRD) patterns were recorded on a Panalytical X'Pert PRO MPD [Cu Kα radiation (λ = 1.5405 Å)], operating at 40 kV and 30 mA. The nitrogen adsorption-desorption isotherms were measured at -196 °C using a Quantochrome Autosorb-1MP sorption analyzer. Samples were degassed under vacuum at 200 °C overnight prior to analysis. X-ray photoelectron spectroscopy (XPS) data were collected with an ESCALab220i-XL electron spectrometer (VG Scientific) using 300 W AlKα radiation. The XPS data were internally standardized with respect to the C 1s peak position at 284.8 eV.

Anode preparation, battery assembly and testing: Slurries of α-Fe_2O_3 hollow microspheres (60% w/w), conductive carbon super P (30% w/w), and PVDF binder (10% w/w) were dispersed in 0.5 mL of NMP and stirred for 10 min. The slurries were doctor-bladed onto a copper foil and dried under vacuum for 12 hr at 80 °C. Circular electrodes (d=15 mm) were punched out of the copper foil, weighed, and subtracted from the copper foil to determine the mass of the active material. The typical mass loading was 0.6 mg/cm^2.

The electrodes were transferred to an argon filled glovebox for coin cell assembly. The cells (model 2032) were fabricated using lithium metal foils as the counter and reference electrodes

and contained an electrolyte mixture of 1.0 M $LiPF_6$ dissolved in ethylene carbonate (EC) and dimethyl carbonate (DMC) (1:1 by volume).

Galvanostatic measurements were made using a LAND CT2001A battery testing system. Cyclic voltammogram curves were examined between 0 – 3 V (vs. Li/Li^+) at a constant scan rate of 2 mV s^{-1}. Cyclability was determined by charging/discharging the cells between 0.05 – 3 V at constant current density of 50 mA g^{-1}. The rate capabilities were determined by charging/discharging at different current densities, according to the sequence: 50, 100, 200, 500, 1000, 50 mA g^{-1}. Capacities are reported based on the mass of α-Fe_2O_3 in the anodes. Electrochemical impedance spectroscopy (EIS) tests were carried out over the frequency ranging from 0.1 to 105 Hz with an ac amplification voltage of 10 mV. After the 50 cycles, the cycled electrodes were disassembled and soaked into acetonitrile for 6h, then rinsed with the ethanol to remove the residual electrolyte, finally drying under 80℃ vacuum.

Table S1. Summary of literature reported lithium battery performance for a number of additive-free* micro/nanostructured α-Fe_2O_3 materials.

a-Fe_2O_3 anode material	Capacity retention (mAh/g)/cycle number (current density (mA/g))	Reference
Nanotubes	1000/50th(500)	[3]
Microboxes	950/30th(200)	[4]
Hollow spheres	710/100th(200)	[5]
Nanorods	970/90th(500)	[6]
Mesoporous nanostructure	1293/50th(200)	[7]
Porous nanorods	1275/30th(100)	[8]
Nanoflakes	680/80th(65)	[9]
Hollow core microspheres	900/100th(150)	[10]
Spindels	1200/10th(100)	[11]
Tuneable porous hematites	1269/50th(50)	[12]
Nanofibers	1293/40th(60）	[13]

* Additive-free denotes batteries assembled without graphene-based additives that are used in addition to binder, electrolyte, and carbon super P used to increase conductivity within coin cells.

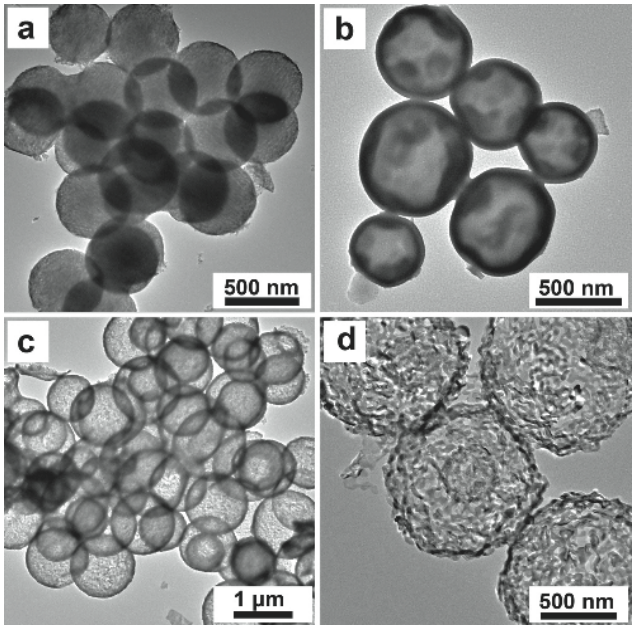

Fig. S1 TEM images of α-Fe_2O_3 multi-shell hollow spheres prepared from carbonaceous microspheres infused with 2.5 M Fe^{2+} ions in solutions of a) pure ethanol, b) 2:1; ethanol: water, c) 1:2; ethanol: water, and d) pure water. All samples were thermally processed at 2°C min^{-1} to 500°C, held for 1 hr, and cooled for 6 hr at room temperature prior to TEM analysis.

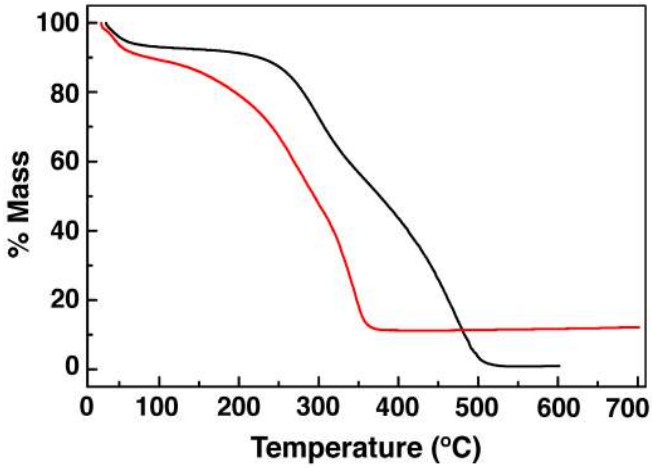

Fig. S2 Thermogravimetric heating curves for thin- (black line) and thick- (red line) shell α-Fe_2O_3 hollow spheres. Experiments were performed under an air atmosphere to mimic standard synthetic conditions.

Table S2. Summary of specific surface area and capacity retention after 50 cycles for α-Fe_2O_3 multi-shell hollow microspheres synthesized with different Fe^{3+} infusion conditions. Specific surface area was calculated from BET data from 0.05 – 0.20 using Quantum software analysis system.

α-Fe_2O_3 Electrode materials	Initial discharge capacity (mA h/g)	First cycle capacity retention (%)	50th capacity retention (mA h/g)	Specific surface area (m^2/g)	Fe^{3+} infusion conditions (Solvent; [Fe^{3+}])
thin 1- shell	2059	75.5	1508	31.6	30ml; 2.5M
thin 2-shell	2187	74.8	1604	37.1	30ml; 3.5M
thin 3-shell	2345	73.5	1702	43.2	30ml; 5.0M
thick 1- shell	1452	74.9	507	20.1	20ml H_2O, 10ml EtOH; 2.5M
thick 2- shell	1502	80.0	429	24.5	20ml H_2O, 10ml EtOH; 3.5M
thick 3- shell	1616	80.8	750	23.7	20ml H_2O, 10ml EtOH; 4.0M
thick 4-shell	1702	82.3	589	29.2	20ml H_2O, 10ml EtOH; 5.0M

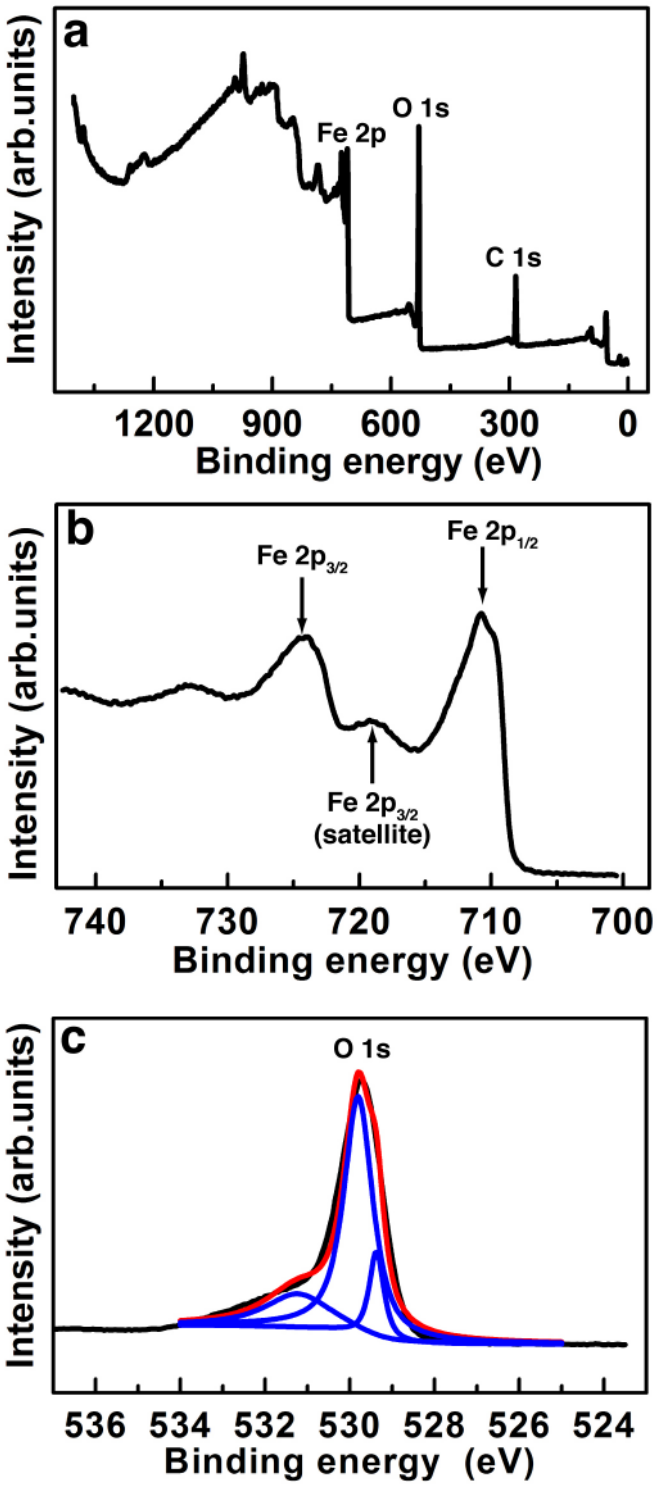

Fig. S3 X-ray photoelectron spectroscopy of thin triple-shell α-Fe_2O_3 hollow spheres: a) the survey scan, and high resolution scans of the b) iron and c) oxygen edges. The data for the oxygen 1s peak (black line) was fit in origin (red line) and deconvoluted into three distinct oxygen species (blue lines).

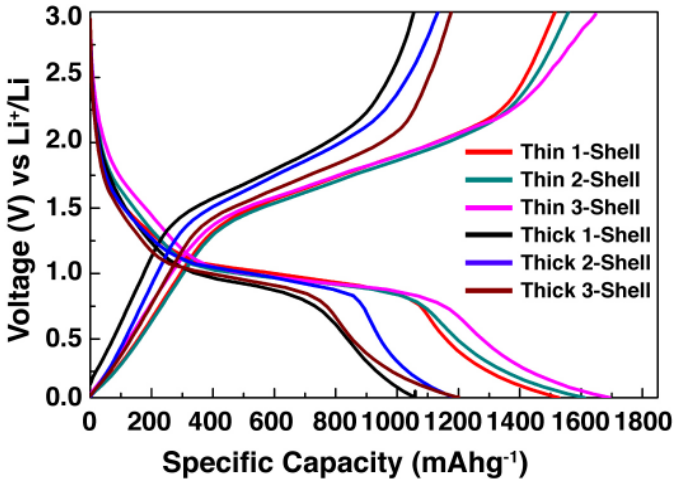

Fig. S4 Comparative voltage profiles at the fifth cycle for thin and thick α-Fe_2O_3 multi-shell hollow spheres at a constant current density of 50 mA g^{-1} between 0.05 – 3 V.

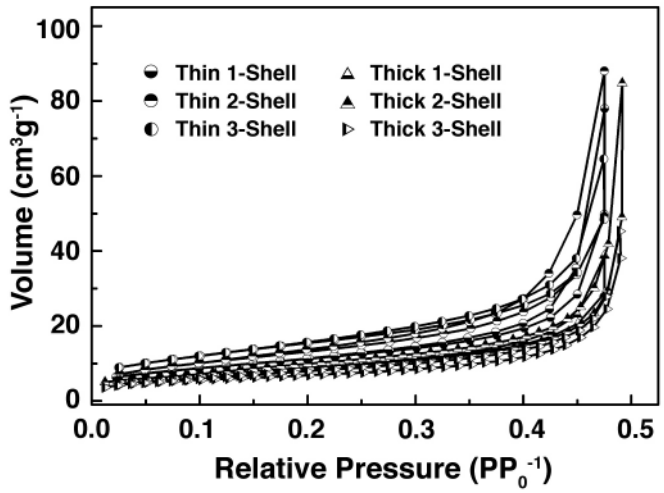

Fig. S5 BET nitrogen adsorption–desorption isotherms for thin and thick α-Fe_2O_3 multi-shell hollow spheres.

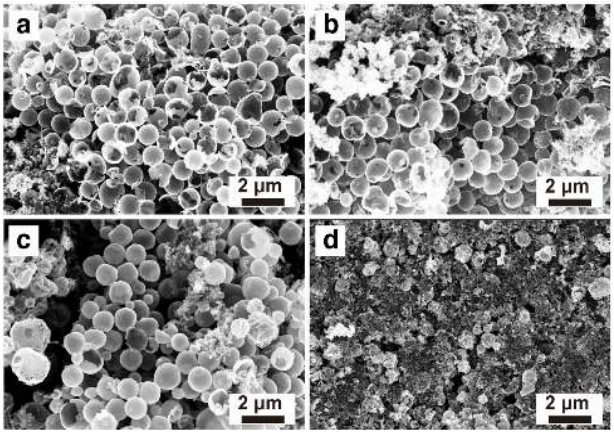

Fig. S6 SEM images of α-Fe_2O_3single-shell hollow microspheres anode films (a) thin- (c) thick-shell after the first lithiation cycle and (b) thin- (d) thick-shell after the final (50^{th}) delithiation cycle. Anode films were recovered after cycling by disassembly of coin cells prior to SEM analysis.

References:

1 X. Sun, Y. Li, *Angew. Chem. Int. Ed.,* 2004, **43**, 597-601.

2 X. Sun, Y. Li, *Chem. Eur. J.,* 2006, **12**, 2039-2047.

3 Z. Wang, D. Luan, S. Madhavi, C. Li, X. W. Lou, *Chem. Commun.,* 2011, **47**, 8061-8063.

4 L. Zhang, H. Wu, S. Madhavi, H. H. Hng, X. W. Lou, *J. Am. Chem. Soc.,* 2012, **134**, 17388-17391.

5 B. Wang, J. Chen, H. Wu, Z. Wang, X. W. Lou, *J. Am. Chem. Soc.,* 2011, **133**, 17146-17148.

6 Y. Lin, P. R. Abel, A. Heller, C. B. Mullins, *J. Phys. Chem. Lett.,* 2011, **2**, 2885-2891.

7 B. Sun, J. Horvat, H. S. Kim, W-S. Kim, J. Ahn, G. Wang, *J. Phys. Chem. C,* 2010, **114**, 18753-18761.

8 X. Yao, C. Tang, G. Yuan, P. Cui, X. Xu, Z. Liu, *Electrochem. Commun.,* 2011, **13**, 1439-1442.

9 M. V. Reddy, T. Yu, C. Sow, Z. Shen, C. T. Lim, G. V. S. Rao, B. V. R. Chowdari, *Adv. Funct. Mater.,* 2007, **17**, 2792-2799.

10 J. Zhong, C. Cao, Y. Liu, Y. Li, W. S. Khan, *Chem. Commun.,* 2010, **46**, 3869-3871.

11 C. Shi, C. Cao, D. Wu, Y. Li, M. Wang, W. Mao, *Mater. Lett.,* 2012, **83**, 35-38.

12 D. Su, H-S. Kim, W-S. Kim, G. Wang, *Microporous Mesoporous Mater.,* 2012, **149**, 36-45.

13 S. Chaudharia, M. Srinivasan, *J. Mater. Chem.,* 2012, **22**, 23049-23056.